

# Cell Death Parameters as Revealed by Whole-Cell Patch-Clamp and Interval Weighted Spectra Averaging: Changes in Membrane Properties and Current Frequency of Cultured Mouse Microglial Cells Induced by Glutaraldehyde

Aleksandar Kalauzi · Ljiljana Nikolić ·  
Danijela Savić · Ksenija Radotić

Received: 15 August 2014 / Accepted: 23 October 2014 / Published online: 4 November 2014  
© Springer Science+Business Media New York 2014

**Abstract** The physiological and biochemical factors that lead to cell death have not been recognized completely. To our knowledge, there are no data on the bioelectric parameters that characterize early period of cell death, as well as on the appearance of related membrane current frequencies. We studied early parameters of glutaraldehyde (GA)-induced cell death, by examining the membrane properties of mouse microglia using the whole-cell patch-clamp technique. In addition, we investigated the GA-induced changes in the membrane current frequency, to see if characteristic frequencies would appear in dying cell. For data analysis, we applied a new approach, an improved multiple moving window length analysis and interval weighted spectra averaging (IWSA). We chose GA for its ability to induce almost instantaneous cell death. The 0.6 % GA did not induce changes in the bioelectric membrane properties of microglia. However, the 3 % GA caused significant decrease of membrane capacitance and resistance accompanied by the prominent increase in the membrane currents and nearly ohmic current response of microglial cells. These data indicate that 3 % GA caused complete loss of the membrane function consequently inducing instantaneous cell death. The membrane function loss was characterized by appearance of the 1.26–4.62 Hz frequency peak in the IWSA spectra, while no significant increase of amplitudes could be observed for cells treated with 0.6 %

GA. To our knowledge, this is the first record of a frequency associated with complete loss of the membrane function and thus can be considered as an early indicator of cell death.

**Keywords** Microglia · Interval weighted spectra averaging · Membrane current frequency · Patch-clamp · Whole-cell current

## Introduction

Cell death is a part of normal development and maturation cycle, and is the component of many response patterns of living tissues to xenobiotic agents (i.e. micro organisms and chemicals) and to endogenous modulations, such as inflammation and disturbed blood supply (Vaux 1993; Kanduc et al. 2002). The physiological and biochemical factors that lead to cell death are still not clear. Also, early parameters of cell death have not been recognized completely. According to the literary data, it emerges that apoptosis and necrosis are two distinct forms of cell death (Renvoize et al. 1998; Martin 2001). These two processes are temporally dislocated and represent the two extremes of a continuum: the necrosis process can start only and exclusively when the cell dies and is an irreversible process, a ‘no return’ way in the cell life (Kanduc et al. 2002).

Glutaraldehyde (GA) is a 5-carbon molecule with two aldehyde functional groups (represented as  $\text{H}-\text{C}=\text{O}$ ), which are highly reactive toward amines. When GA comes in interaction with proteins’ amino groups, it cross-links the proteins. This inactivates proteins and cross-links/immobilizes cells (Migneault et al. 2004; McGuinley 2012). GA is the most effective crosslinking agent, which is the reason for its use in histo- and cytochemistry (Sabatini et al. 1963; Anderson 1967), microscopy (Sabatini et al. 1963; Hayat

---

A. Kalauzi · K. Radotić (✉)  
Institute for Multidisciplinary Research, University of Belgrade,  
Kneza Višeslava 1, 11000 Belgrade, Serbia  
e-mail: xenia@imsi.rs

L. Nikolić · D. Savić  
Institute for Biological Research “Siniša Stanković”, University  
of Belgrade, Bulevar Despota Stefana 142, 11000 Belgrade,  
Serbia

1981; Kiernan 2000), enzyme technology (Quioco and Richards 1966; Richards and Knowles 1968; Fishman et al. 1971), chemical sterilization (Gorman et al. 1980), and biomedical (Nimni et al. 1987) and pharmaceutical sciences (Gosselin et al. 1976). As most cross-linkers, GA has no specificity toward a given class of proteins. However, it is undisputed that GA is specific for cross-linking mainly the free amino groups of lysine (Korn et al. 1972). Most proteins contain many lysine residues, usually located on the protein surface (i.e., exposed to the aqueous medium) because of the polarity of its amine group.

We studied early parameters of GA-induced cell death, by examining the membrane properties of cultured mouse microglia using the whole-cell patch-clamp technique. In addition, we investigated the GA-induced changes in the membrane current frequency, intending to see if characteristic membrane current frequencies would appear in dying cell. For data analysis, we applied a new approach, an improved multiple moving window length analysis and Interval Weighted Spectra Averaging (IWSA). We chose GA for its ability to induce almost instantaneous cell death, due to the strong protein cross-linking mechanism. To our knowledge, there are no data on the bioelectric parameters that characterize early period of cell death, as well as on the appearance of related frequencies in the membrane current.

## Materials and Methods

### Primary Microglia Cultures

Mixed cortical cultures from newborn C57BL/6 mice (day 0–3) were made according to the procedure described previously (Giulian and Baker 1986). Cultures were kept in Dulbecco's modified Eagle's medium (Gibco), supplemented with 10 % heat-inactivated fetal calf serum (PAA), and 1 % penicillin/streptomycin (PAA). Ten days after plating, primary microglia were detached from the astrocytes by gentle shaking. Microglial cells were plated at  $2 \times 10^4$  on glass cover slips ( $\varnothing 18$  mm) in 35-mm dishes with 2 ml of astrocyte-conditioned medium. After 24 h of culture, microglial cells were used for experiments.

### Whole-Cell Patch-Clamp Recordings

Electrophysiological recordings from cultured mouse microglia were obtained with the whole-cell configuration of the patch-clamp technique (Hamill et al. 1981). A coverslip with plated cells was placed in the recording chamber on the stage of Olympus BH2 upright microscope (Olympus, Center Valley, PA, USA). Patch-clamp recordings were performed using Tecella Pico 2 amplifier with

TecellaLab software (Tecella, Foothill Ranch, CA, USA). Extracellular solution (ECS) consisted of (in mM) 4KCl, 140NaCl, 2MgCl<sub>2</sub>, 2CaCl<sub>2</sub>, 10 HEPES, 5 glucose and pH 7.4 adjusted with NaOH (Sigma-Aldrich, Taufkirchen, Germany). Patch pipettes made from borosilicate glass capillaries of 1.5 mM outer and 0.86 mM inner diameter (Science Products, Hofheim, Germany) had resistance of 4–6 M $\Omega$  when filled with intracellular solution of the following composition (in mM): 144KCl, 2MgCl<sub>2</sub>, 5 EGTA and 10 Hepes, pH 7.2 adjusted with KOH (Sigma). Membrane currents were low-passed filtered at 2 kHz and digitized at 20 kHz using Tecella Pico2 amplifier with integrated digitizer (Tecella). Membrane resistance ( $R_m$ ) and capacitance ( $C_m$ ) were measured directly from the amplifier. Whole-cell currents were evoked by stepping the holding potential of  $-50$  mV from  $-150$  to  $+70$  mV in 20 mV increments. During registration in the gap-free voltage-clamp mode, the membrane potential was clamped at  $-50$  mV. All recordings were obtained at room temperature ( $22^\circ\text{C}$ ). GA (25 % EM GRADE, Agar Scientific LTD, Essex, UK) was added directly to the recording chamber at the final concentrations of 0.6 or 3 %. To verify the effect of GA, the membrane properties of microglia were also examined after addition of the same volume of ECS. Currents evoked by voltage step and gap-free protocols were analyzed in Clampfit software (Axon Instruments, Sunnyvale, CA, USA). Current densities were calculated by dividing the amplitude of evoked current by  $C_m$ . Step current densities in the control condition and in the presence of GA were divided by the maximum control current density (at  $+70$  mV step) for each cell ( $I/I_{\text{max}}$ ). The current density in the gap-free mode was measured as the difference in the current level between the control and GA conditions.  $C_m$  and  $R_m$  values in GA were normalized to the corresponding control values within each experiment. Data were plotted and analyzed using SigmaPlot (Systat Software Inc., San Jose, CA, USA). The differences between the compared groups were considered significant for  $p < 0.05$ . Data are presented as mean  $\pm$  SEM.

### Data Analysis

For each cell, current responses of 10 s duration obtained in gap-free mode were subjected to FFT analysis. However, since a signal of limited duration was analyzed, we employed an improved multiple moving window length analysis and IWSA, devised for this purpose. In principle, different amplitude spectra could be obtained with different moving FFT window lengths, where frequency resolution is directly proportional, while the number of available spectra is inversely proportional to the window duration. With 10 s signal epochs, the finest resolution (0.1 Hz)

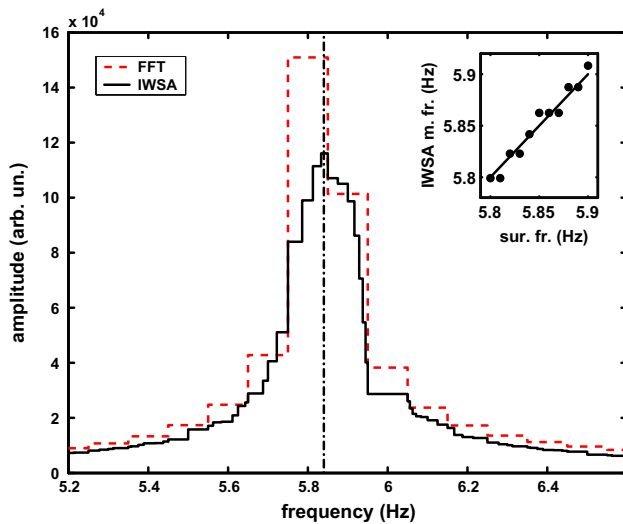


**Fig. 1** Example of increased accuracy of the IWSA method on the surrogate 5.84 Hz sinusoid of 10 s duration. Conventional 0.1 Hz frequency resolution FFT amplitude spectrum (red dashed line); IWSA spectrum (black solid line); exact sinusoid frequency 5.84 Hz (vertical dash-dot line). Inset: (filled circle) Results of the application of IWSA method on a set of surrogate sinusoids with frequencies 5.80, 5.81, ..., 5.90 Hz. Surrogate sinusoid frequency (sur. fr., abscissa); frequency where maximal IWSA amplitude was detected (IWSA m. fr., ordinate) (Color figure online)

resulted from application of one window on the whole signal. However, by varying window duration from 1 to 10 s, while keeping the window step constant (0.1 s), we were able to generate series of ten amplitude spectra for each cell and each experimental condition (control, 0.6 and 3 % GA). Next, spectra from each series were used to yield one IWSA spectrum according to the following procedure. As each window of duration  $d$  induces a different partitioning of the frequency axis, let  $f_{d_j}^i$ ,  $i = 1, \dots, n_d$ , be the set of frequency interval limits, where  $n_d$  stands for their number. Let us now observe a combined uneven partition, by forming a union of sets of all interval limits, where repeated limits were eliminated:

$$f_{d_1, d_N}^k = \bigcup_{j=1}^N f_{d_j}^i, f_{d_1, d_N}^k \neq f_{d_1, d_N}^l$$

where  $d_1, \dots, d_N$  represent window durations,  $i = 1, \dots, n_d$ , while  $k$  and  $l$  stand for indexes of members of the united set. If a spectrum corresponds to a moving window of duration  $d_j$ , we shall say that amplitude  $A_{d_j}^i$  is spreading over the interval  $[f_{d_j}^i, f_{d_j}^{i+1}]$ . Generally, since amplitude  $A_{d_j}^i$  may be spreading over more combined intervals  $[f_{d_1, d_N}^k, f_{d_1, d_N}^{k+1}]$ , with  $A_{d_j}^{k, k+1}$  we shall denote that  $A_{d_j}^{k, k+1} = A_{d_j}^i$ ,

if  $[f_{d_1, d_N}^k, f_{d_1, d_N}^{k+1}] \subset [f_{d_j}^i, f_{d_j}^{i+1}]$ . The IWSA procedure was then performed according to the formula

$$A_{d_1, d_N}^{k, k+1} = \frac{\sum_{j=1}^N A_{d_j}^{k, k+1} \frac{1}{f_{d_j}^{i+1} - f_{d_j}^i}}{\sum_{j=1}^N \frac{1}{f_{d_j}^{i+1} - f_{d_j}^i}}.$$

In other words, the resulting IWSA amplitude at a particular frequency point is obtained as a weighted average of Fourier amplitudes calculated for all frequency intervals containing that point, whereas inverse interval lengths serve as the weighting factors. Using IWSA on a set of surrogate sinusoids where frequencies were evenly spaced at  $10^{-2}$  Hz (5.80, 5.81, ..., 5.90 Hz), we were able to increase the accuracy roughly for an order of magnitude (please see Fig. 1, where classical FFT with 0.1 Hz resolution could yield only 5.8 or 5.9 Hz as a result).

## Results

### Electrophysiological Measurements (Whole-Cell Patch-Clamp)

Application of GA at the 0.6 % concentration did not cause noticeable changes in the measured membrane parameters of microglial cells (Fig. 2,  $n = 3$ ). It can be seen that the whole-cell step current responses were not noticeably changed after addition of 0.6 % GA (Fig. 2a). Furthermore, current densities obtained in control and 0.6 % GA and plotted against the stepped membrane potentials had similar profile (Fig. 2a, right panel). In addition, 0.6 % GA induced small and non-significant increase of  $C_m$  and  $R_m$  values in examined cells (Fig. 2b).

However, application of a higher 3 % GA concentration caused prominent changes in all examined membrane parameters of microglia (Fig. 3,  $n = 3$ ). The whole-cell step current responses were prominently changed by 3 % GA (Fig. 2a). Thus, after addition of 3 % GA, the obtained I-V plot became nearly ohmic. Accordingly, the current densities were significantly increased by 3 % GA as estimated at the  $-110$  and  $+30$  mV steps (Fig. 3a, right panel). Moreover, the  $C_m$  and  $R_m$  parameters were significantly decreased by 3 % GA (Fig. 3b).

Next, we examined changes in the whole-cell currents recorded from microglia induced by 0.6 % and subsequently applied 3 % GA in the gap-free mode. We observed that 0.6 % GA induced small non-significant change in the whole-cell current recorded from microglia (Fig. 4a). However, 3 % GA induced a prominent and significant current change, again indicating that the microglia membrane is damaged after application of GA at higher concentration (Fig. 4a). The observed changes in the whole-cell current recorded from microglial membrane

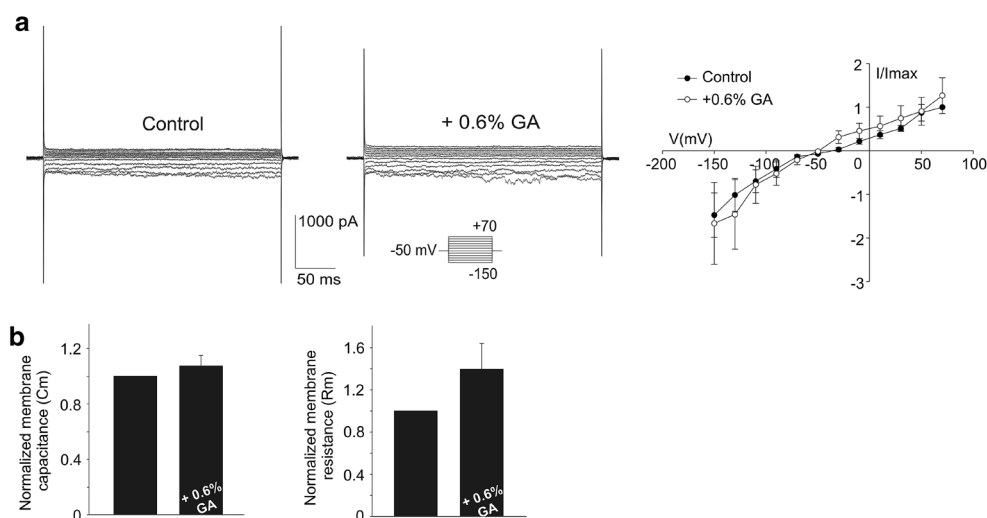


**Fig. 2** Effect of 0.6 % glutaraldehyde (GA) on the whole-cell current response and membrane properties of cultured microglial cells. **a** Examples of voltage step current responses of microglia in the control condition and in the presence of 0.6 % GA. Corresponding normalized current density ( $I/I_{max}$ )–voltage curves illustrate that 0.6 % GA did not induce changes in the inward and outward current

recorded from microglia ( $p > 0.05$ , paired  $t$  test,  $n = 3$ ). Voltage protocol is indicated in the *inset*. **b** The normalized membrane capacitance ( $C_m$ ) and membrane resistance ( $R_m$ ) values were not significantly changed in the presence of 0.6 % GA ( $p > 0.05$ , paired  $t$  test and Wilcoxon test,  $n = 3$ )

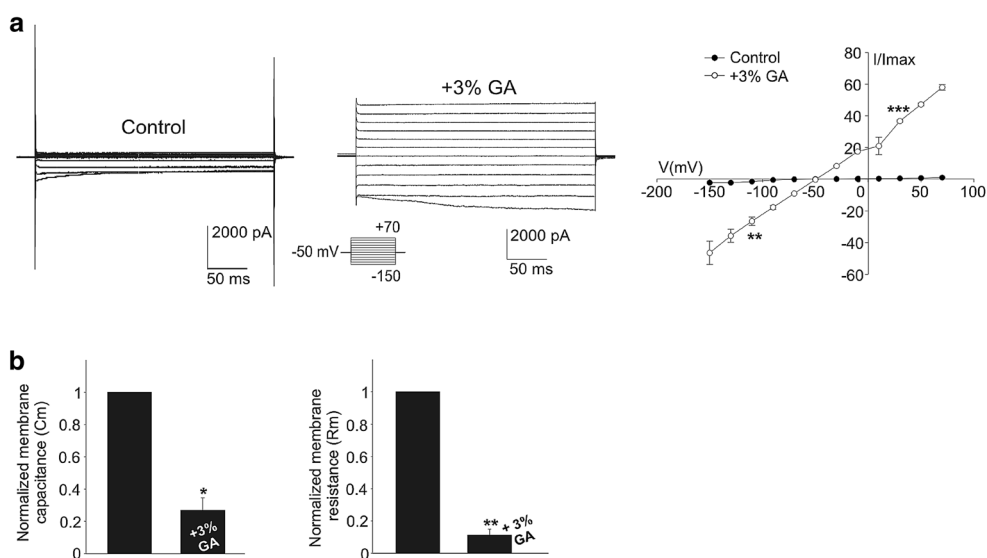


**Fig. 3** Effect of 3 % glutaraldehyde (GA) on the whole-cell current response and membrane properties of cultured microglia. **a** Examples of voltage step current response of microglia in the control condition and in the presence of 3 % GA depict prominent changes in the amplitudes of recorded currents. Corresponding normalized current density ( $I/I_{max}$ )–

voltage curves depict significant augmentation of both inward and outward current densities (\*\* $p < 0.01$ , paired  $t$  test; \*\*\* $p < 0.001$ , paired  $t$  test,  $n = 3$ ). **b** In the presence of 3 % GA, normalized membrane capacitance ( $C_m$ ) and membrane resistance ( $R_m$ ) are significantly diminished (\* $p < 0.05$ , paired  $t$  test, \*\* $p < 0.01$ , paired  $t$  test,  $n = 3$ )

can be attributed to the effect of GA only, since application of the same volume of ECS did not induce any change in the whole-cell current (Fig. 4b).

#### Interval Weighted Spectra Averaging

Difference between IWSA amplitude spectra of the whole-cell current signals from the three cells treated with 3 %

GA and in control condition is presented on Fig. 5, as well as their analogous differential IWSA spectra between signals obtained after application of 0.6 % GA and control.

No significant increase of amplitudes could be observed in case of cells treated with 0.6 % GA and control (Fig. 5, blue line). However, when 3 % GA was applied, three frequency regions could roughly be observed: 0–1.26, 1.26–4.62, and 4.62–20 Hz (Fig. 5, red line). In the first

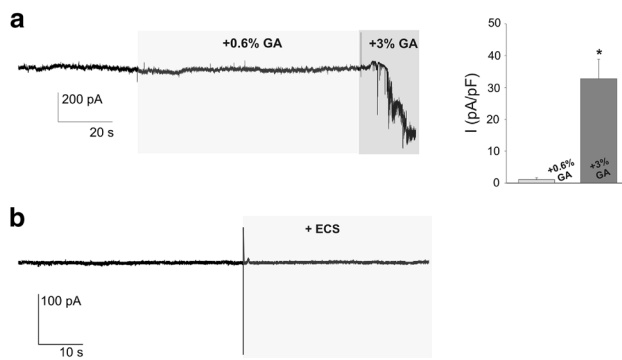


**Fig. 4** Effect of 0.6 and subsequently applied 3 % glutaraldehyde (GA) on the whole-cell currents of cultured microglial cells. **a** Example of the whole-cell current trace of microglia recorded in the gap-free mode illustrates effects of 0.6 % (depicted by light-gray color) and 3 % GA (depicted by dark-gray color). Addition of 0.6 % GA induced small and non-significant change in the whole-cell current density, while the change in the current density induced by the subsequent addition of 3 % GA was prominent and significant ( $p < 0.05$ , paired  $t$  test,  $n = 4$ ). **b** Addition of extracellular solution (ECS, depicted by light-gray color) did not alter the whole-cell current recorded from microglia ( $n = 3$ ) (Color figure online)

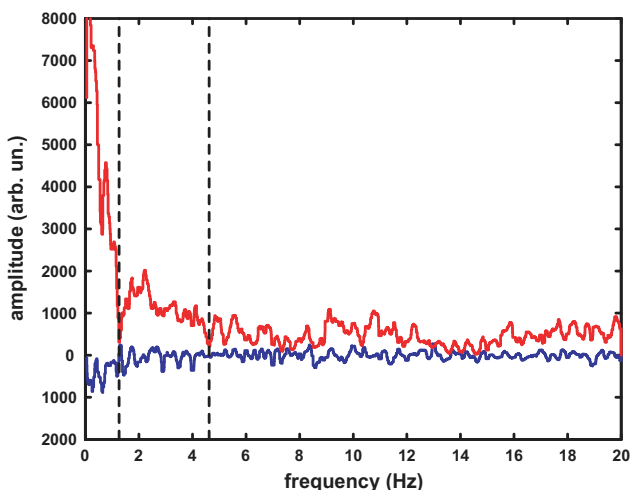


**Fig. 5** Difference of IWSA amplitude spectra between cells treated with 3 % GA and control (red). Analogous spectra for difference between cells treated with 0.6 % GA and control (blue) (Color figure online)

two regions, IWSA amplitudes were prominently increased, while in the range of higher frequencies the increase, although present, was less noticeable. When IWSA amplitudes, averaged across the corresponding frequency regions for each cell, were tested with Wilcoxon Signed ranks Test and Mann–Whitney U Test (IBM SPSS Statistics 20), no significant increases were found (Table 1). However, when frequency averaged data for the additional two cells treated only with 3 % GA were added, both tests, for the ensemble of five cells, found significant increases in regions 0–1.26 and 1.26–4.62 Hz (Table 1).

## Discussion

Changes in analyzed electrophysiological parameters of microglial cells indicated that 0.6 % GA induced small and non-significant changes, while 3 % GA damaged the cell membrane, consequently causing the death of microglial cells. Nearly ohmic I–V plot after addition of 3 % GA clearly illustrates instantaneous cell death due to the complete loss of the membrane function. In a previous study (Margineanu and Van Driessche 1990), the effects of millimolar concentrations of GA on the electrophysiological properties of the epithelium tissue of the frog skin (*Rana temporaria*) were investigated. At concentrations above 0.005 % (w/v) or 0.5 mM, GA irreversibly and completely inhibited both  $I_{Na}$  and  $I_K$  within 2–3 h. Prolonged exposure to millimolar concentrations of GA resulted in a large increase in the chloride permeability of the frog skin. Our results show that addition of 60 mM (0.6 %) GA does not cause significant changes in the membrane properties and whole-cell currents of cultured microglial cells. In addition, data obtained in this study indicate that 300 mM (3 %) GA application caused the loss of membrane function as evidenced from prominent changes in the membrane resistance and capacitance, and whole-cell current response of microglial cells. The difference between our and results obtained in previous study (Margineanu and Van Driessche 1990) may be attributed to the differences between experimental objects examined. In fact, cellular interactions may be responsible for the observed effects of GA described on the epithelium of the frog skin. In this study, we have investigated the response of single microglial cells to GA thus excluding the interaction between the cells. By analyzing additional membrane parameters, we found that membrane capacitance was not considerably changed after 0.6 % GA treatment, while large decrease in the cell membrane capacitance after 3 % GA application was detected. Such drastic capacitance changes may be due to the GA-induced cross-linking of the ion channel proteins (Migneault et al. 2004) and thus lose of membrane integrity.

Further analysis of membrane current frequencies by using IWSA method showed that 1.26–4.62 Hz peak may be a strong candidate for an early parameter of cell death. While additional measurements are needed to identify origins of the differences in the two regions, we are less convinced that the lowest frequency region (0–1.26 Hz) contains biologically relevant oscillations, since both linear and non-linear signal trends tend to appear in the region of lowest frequencies. Although we applied detrending prior to FFT, this procedure removed only simple linear trends, while more complex multilinear and non-linear trends remained, as their removal would request a mathematical modeling approach on the case-to-case basis. Moreover,



**Table 1** Results of statistical tests between averaged IWSA amplitudes across three frequency ranges in control condition, after application of 0.6 and 3 % glutaraldehyde

Three cells	Frequency range (Hz)					
	0–1.26		1.26–4.62		4.62–20	
	Control vs. 0.6 % glutarald	Control vs. 3 % glutarald	Control vs. 0.6 % glutarald	Control vs. 3 % glutarald	Control vs. 0.6 % glutarald	Control vs. 3 % glutarald
Wilcoxon signed ranks	$Z = -1.604$ $p = 0.109$	$Z = -1.604$ $p = 0.109$	$Z = -1.604$ $p = 0.109$	$Z = -1.604$ $p = 0.109$	$Z = 0.000$ $p = 1.000$	$Z = -1.604$ $p = 0.109$
Mann–Whitney	$Z = -0.655$ $p = 0.513$	$Z = -1.528$ $p = 0.127$	$Z = -0.655$ $p = 0.513$	$Z = -1.091$ $p = 0.275$	$Z = -0.218$ $p = 0.827$	$Z = -1.091$ $p = 0.275$
Five cells	Frequency range [Hz]					
	0–1.26		1.26–4.62		4.62–20	
	Control vs. 3 % glutarald		Control vs. 3 % glutarald		Control vs. 3 % glutarald	
Wilcoxon Signed Ranks	$Z = -2.023$ <b><math>p = 0.043</math></b>		$Z = -2.023$ <b><math>p = 0.043</math></b>		$Z = -1.604$ $p = 0.109$	
Mann–Whitney	$Z = -2.402$ <b><math>p = 0.016</math></b>		$Z = -1.984$ <b><math>p = 0.047</math></b>		$Z = -1.776$ $p = 0.076$	

Significant differences are bolded ( $p < 0.05$ )

relative sharpness of IWSA amplitude peaks (as the one appearing at 0.75 Hz) could point to a technical source. On the other hand, the medium region peak (1.26–4.62 Hz) remains to be a stronger candidate for the one generated by damaged cells, according to its positive orientation and dispersed (smeared) shape, typical for oscillations of biological origin. As we reported in our previous work (Kalauzi et al. 2012), dispersed amplitude peaks could be explained either by multiple frequency oscillations or one carrier frequency oscillation whose amplitude, (as well as frequency or phase) was modulated by lower frequencies. Since the medium region (1.26–4.62 Hz) peak is a strong candidate for being generated by damaged cells, according to its typically dispersed shape, this frequency may be considered as an early indicator of cell death. To our knowledge this is the first record of a frequency associated with complete loss of membrane function. However, exact cellular and molecular mechanisms responsible for its generation are yet to be elucidated.

## Conclusion

In the present study, we have shown that mouse microglia cell death caused by 3 % GA is characterized by prominent changes in the membrane properties and almost passive membrane current response, as well as by the appearance of the membrane current frequencies in the 1.26–4.62 Hz range.

**Acknowledgments** This work was supported by the Grants III45012, III41014, OI 173022, from the Ministry of Education,

Science and Technological Development of the Republic of Serbia. The authors are grateful to Sutter Instrument Company for donating the MP-285 Micromanipulator System, and Tecella Company for donating the Tecella Pico 2 amplifier.

## References

- Anderson PJ (1967) Purification and quantitation of glutaraldehyde and its effect on several enzyme activities in skeletal muscle. *J Histochem Cytochem* 15:652–661
- Fishman SN, Chodorov BI, Volkenstein MV (1971) Molecular mechanisms of membrane ionic permeability changes. *Biochim Biophys Acta* 225:1–10
- Giulian D, Baker J (1986) Characterization of ameboid microglia isolated from developing mammalian brain. *J Neurosci* 6:2163–2178
- Gorman SP, Scott EM, Russell AD (1980) Antimicrobial activity, uses and mechanism of action of glutaraldehyde. *J Appl Bacteriol* 48:161–190
- Gosselin RE, Hodge HC, Smith RP, Gleason MN (1976) *Clinical Toxicology of Commercial Products. Acute Poisoning*, 4th edn. The Williams & Wilkins Co., Baltimore
- Hamill O, Marty A, Neher E, Sakmann B, Sigworth F (1981) Improved patch-clamp techniques for high-resolution current recording from cells and cell-free membrane patches. *Pflugers Arch* 391:85–100
- Hayat MA (1981) *Fixation for Electron Microscopy*. Academic Press, New York
- Kalauzi A, Vučković A, Bojić T (2012) EEG alpha phase shifts during transition from wakefulness to drowsiness. *Int J Psychophysiol* 86:195–205
- Kanduc D, Mittelman A, Serpiko R, Sinigaglia E, Sinha AA et al (2002) Cell death: apoptosis versus necrosis. *Int J Oncol* 21:165–171
- Kiernan JA (2000) Formaldehyde, formalin, paraformaldehyde and glutaraldehyde: what they are and what they do. *Microsc Today* 00:1:8–12

- Korn AH, Fearheller SH, Filachione EM (1972) Glutaraldehyde: nature of the reagent. *J Mol Biol* 65:525–529
- Margineanu D-G, Van Driessche W (1990) Effects of millimolar concentrations of glutaraldehyde on the electrical properties of frog skin. *J Physiol* 427:567–581
- Martin LJ (2001) Neuronal cell death in nervous system development, disease, and injury. *Int J Mol Med* 7:455–478
- McGuinley HR (2012) Glutaraldehyde uses and counterfeits. *Water Technology* (2012) <http://www.watertechonline.com/articles/165425-glutaraldehyde-uses-and-counterfeits> pp 30–32
- Migneault I, Dartiguenave C, Bertrand MJ, Waldron KC (2004) Glutaraldehyde: behavior in aqueous solution, reaction with proteins, and application to enzyme crosslinking. *Biotechniques* 37:790–802
- Nimni ME, Cheung D, Strates B, Kodama M, Sheikh K (1987) Chemically modified collagen: a natural biomaterial for tissue replacement. *J Biomed Mater Res* 21:741–771
- Quioco FA, Richards FM (1966) The enzymic behavior of carboxypeptidase-A in the solid state. *Biochemistry* 5:4062–4076
- Renvoize C, Biola A, Pallardy M, Breard J (1998) Apoptosis: identification of dying cells. *Cell Biol Toxicol* 14:111–120
- Richards FM, Knowles JR (1968) Glutaraldehyde as a protein cross-linkage reagent. *J Mol Biol* 37:231–233
- Sabatini DD, Bensch K, Barnett RJ (1963) Cytochemistry and electron microscopy. The preservation of cellular ultrastructure and enzymatic activity by aldehyde fixation. *J Cell Biol* 17:19–58
- Vaux DL (1993) Toward an understanding of the molecular mechanisms of physiological cell death. *Proc Natl Acad Sci USA* 90:786–789